

Gravitational-wave constraints on the GWTC-2 events by measuring the tidal deformability and the spin-induced quadrupole moment

Tatsuya Narikawa^{1,*}, Nami Uchikata^{1,†} and Takahiro Tanaka^{2,3‡}

¹*Institute for Cosmic Ray Research,
The University of Tokyo, Chiba 277-8582, Japan*

²*Department of Physics,
Kyoto University, Kyoto 606-8502, Japan*

³*Center for Gravitational Physics,
Yukawa Institute for Theoretical Physics,
Kyoto University, Kyoto 606-8502, Japan*

(Dated: September 28, 2021)

Gravitational waves from compact binary coalescences provide a unique laboratory to test properties of compact objects. As alternatives to the ordinary black holes in general relativity, various exotic compact objects have been proposed. Some of them have largely different values of the tidal deformability and spin-induced quadrupole moment from those of black holes, and their binaries could be distinguished from the binary black hole by using gravitational waves emitted during their inspiral regime, excluding the highly model-dependent merger and ringdown regimes. We reanalyze gravitational waves from low-mass merger events in the GWTC-2, detected by the Advanced LIGO and Advanced Virgo. Focusing on the influence of tidal deformability and spin-induced quadrupole moment in the inspiral waveform, we provide model-independent constraints on deviations from the standard binary black hole case. We find that all events that we have analyzed are consistent with the waveform of the binary black hole in general relativity. Bayesian model selection shows that the hypothesis that the binary is composed of exotic compact objects is disfavored by all events.

I. INTRODUCTION

Gravitational waves (GWs) that are thought to originate from binary black hole (BBH) coalescences have been detected with the Advanced LIGO and Advanced Virgo interferometers [1, 2]. General relativity (GR) has been tested using GWs from compact binary coalescences in several ways [3].

Exotic compact objects (ECOs), such as boson stars, gravastars, wormholes, and some models of quantum corrections at around the horizon, have been proposed as alternatives to the black holes (BHs) of classical GR (see Ref. [4] for review). Some proposed ECOs have largely different values of the tidal deformability and spin-induced quadrupole moment (SIQM) from those of BHs in GR. The inspiral regime for GW signals emitted from binary ECOs can be characterized through the tidal deformability [5–9] and SIQM [5, 10]. Therefore, their binaries could be distinguished from BBHs by using GWs.

Tidal deformability and SIQM can also characterize the equation-of-state (EOS) for a neutron star (NS). For the binary-neutron-star mergers, most analyses of GW170817 and GW190425 focus on measuring the tidal deformability using the EOS-insensitive relations between tidal deformability and SIQM called Love-Q relations predicted by theoretical studies [11–17].

Regarding the tidal absorption effects [18–21], some

studies have proposed that some ECOs such as boson stars do not absorb GWs efficiently [20, 22–24] (see Ref. [4] for review). In this paper, we ignore the tidal absorption effects because of uncertainty of theoretical understanding, e.g., uncertainty of frequency dependence on horizon energy flux [25].

At the very late inspiral regime, the tidal resonance for binary ECO systems is also modeled in Ref. [26], and resonant excitations in ECOs have been constrained via GWTC-1 events [27]. At postmerger regimes for binary ECO, emission of GW echoes following normal inspiral-merger-ringdown signal have been proposed and have been searched [28–30]. A toy model for postcontact regimes of binary ECOs has been recently introduced [31]. In this paper, we do not consider the postinspiral regimes, such as the resonance and GW echoes.

Previous studies regarding real data analysis of GWs to test ECO hypothesis have considered only the effect of either the tidal deformability or the SIQM on the signal, and the BH's value for the other parameter has been used. The studies focusing on the SIQM effect alone have been done in Refs. [32–36]. In particular, Krishnendu *et al.* have constrained the properties of GW151226 and GW170608 from the measurements of SIQM [36], and the paper on tests of GR by the LIGO Scientific Collaboration and the Virgo Collaboration (LVC) has constrained the ECO hypothesis with the GWTC-2 events [3]. The studies focusing on the tidal effect alone have been done in Refs. [37–40]. In particular, Johnson-Mcdaniel *et al.* have tested how well BH mimickers with polytropic EOS are constrained by measuring tidal deformabilities via injected O1 BBH-like events [40]. They show future

* narikawa@icrr.u-tokyo.ac.jp

† uchikata@icrr.u-tokyo.ac.jp

‡ t.tanaka@tap.sphys.kyoto-u.ac.jp

prospects of detection of deviations from GR assuming boson stars. We note, however, that the above works do not consider both effects simultaneously but focus on only one of them.¹

The aim of this work is to give model-independent tests of strong-field gravity regimes from the measurements of tidal deformability and SIQM via GWs from compact binary inspirals. One motivation to think about BH mimickers is to modify the BHs in GR to be compatible with the stringy paradigm as to BH information loss. If we assume something like a firewall, only the small region near the horizon might be modified, or in other words practically only the absorbing boundary condition across the horizon might be modified. This change of boundary condition may also result in the modification of tidal deformability, unless the modification is restricted to a really tiny region in the vicinity of the horizon, e.g., within the Planck distance from the horizon. (Thus, we think nontrivial tidal deformability will not necessarily imply smaller compactness.)

In this paper, we reanalyze the data around six low-mass events identified as BBH; GW151226, GW170608, GW190707.093326 (hereafter GW190707), GW190720.00836 (hereafter GW190720), GW190728.064510 (hereafter GW190728), and GW190924.021846 (hereafter GW190924), using an inspiral-only waveform model with both tidal and SIQM terms, and present constraints on the binary tidal deformability and SIQM at the same time. We focus on the inspiral regime because postinspiral regimes of binary ECOs are not modeled well. Since the inspiral regime can be accurately described by the post-Newtonian (PN) formula [5, 42, 43], we use the PN inspiral-only waveform model.

The remainder of this paper is organized as follows. In Sec. II, we explain the methods of Bayesian parameter estimation for GWs including waveform models used to analyze. In Sec. III, we present results of our analysis of GWTC-2 events by using `TF2g_Tidal_SIQM` waveform model. Section IV is devoted to a summary and conclusion. In Appendix A, we show the results for seven events added GW190814 by using the `TF2.Tidal_SIQM` waveform model. Here, `TF2` is the abbreviation of `TaylorF2`, which is the PN waveform model for point-particle and spin effects [42, 44, 45], and `TF2g` is an extended waveform model of `TF2` obtained by Taylor-expanding the effective-one-body formula [46].

We employ the units $c = G = 1$, where c and G are the speed of light and the gravitational constant, respectively.

II. PARAMETER ESTIMATION METHODS

A. ECO features

There are several features of ECOs that differ from BH (see Refs. [4] for review). In this paper, we focus on the tidal deformability and SIQM.

1. Tidal deformability

In the compact binary inspiral, at the leading order, the tidally induced quadrupole moment tensor $Q_{ij,\text{Tidal}}$ is proportional to the companion's tidal field \mathcal{E}_{ij} as $Q_{ij,\text{Tidal}} = -\lambda\mathcal{E}_{ij}$. The information about the EOS (or structure) can be quantified by the tidal deformability parameter λ [6]. The leading-order tidal contribution to the GW phase evolution (relative 5PN order) arises through the symmetric contribution of tidal deformation, the binary tidal deformability [6, 7, 47]

$$\tilde{\Lambda} = \frac{16}{13} \frac{(m_1 + 12m_2)m_1^4\Lambda_1 + (m_2 + 12m_1)m_2^4\Lambda_2}{(m_1 + m_2)^5}, \quad (1)$$

which is a mass-weighted linear combination of the both component tidal parameters, where $m_{1,2}$ is the component mass and $\Lambda_{1,2}$ is the dimensionless tidal deformability parameter of each object defined as $\Lambda_{1,2} = \lambda_{1,2}/m_{1,2}^5$. For the waveform models used in this paper, the tidal effects to the gravitational-wave phase are dominated by the symmetric contributions, $\tilde{\Lambda}$ terms, and the anti-symmetric contributions, $\delta\tilde{\Lambda}$ terms, are always subdominant [48, 49]. The tidal deformability can characterize the compact objects. Λ for BHs in classical GR vanishes as shown for a Schwarzschild BH [50, 51] and for Kerr BH [52–54]. For NSs, Λ is a few hundred, depending on the EOS [8, 47, 55–57]. The upper bound on the binary tidal deformability $\tilde{\Lambda}$ by GW170817 is about 900 [13, 58] (see also Refs. [16, 17] for reanalysis). ECOs differ from BHs in classical GR in having nonzero tidal deformabilities [38, 39, 59]. It is intriguing that Λ is negative for gravastars [60, 61].

2. SIQM

For a compact object with mass m and the dimensionless spin parallel to the orbital angular momentum, $\chi = S/m^2$, where S is the magnitude of the spin angular momentum of the aligned component, the spin-induced quadrupole moment scalar is given by [10]

$$Q_{\text{Spin}} = -(1 + \delta\kappa)\chi^2 m^3, \quad (2)$$

where $\delta\kappa$ denotes deviations from the Kerr BHs in GR. The symmetric combination of the deviation parameters of the respective objects, $\delta\kappa_s$, is defined as $\delta\kappa_s = (\delta\kappa_1 + \delta\kappa_2)/2$. The SIQM can also characterize the compact objects. For Kerr BH, we have $\delta\kappa = 0$ [10]. For spinning

¹ The analysis in Ref. [41] has considered both effects at one time for Fisher information matrix analysis.

NS, we have $\delta\kappa \sim 2 - 20$ [62–64]. ECOs differ from BHs, having $\delta\kappa \neq 0$: $\delta\kappa \sim 10 - 150$ for spinning boson stars [65–68]. Interestingly, $\delta\kappa$ for a gravastar can take negative values [61].

B. Waveform models for inspiraling exotic compact objects

We use the PN waveform model, which can accurately describe the early inspiral regime for compact binary coalescences [5, 42]. The frequency-domain gravitational waveform for binary ECOs can be written as

$$\tilde{h}_{\text{ECO}}(f) = A(f)e^{i\Psi_{\text{BBH}}(f) + \Psi_{\text{SIQM}}(f) + \Psi_{\text{Tidal}}(f)}, \quad (3)$$

where $A(f)$ is the amplitude of the GW signal and the phase which consists of the BBH phase $\Psi_{\text{BBH}}(f)$ and the additional SIQM effect $\Psi_{\text{SIQM}}(f)$ and tidal effect $\Psi_{\text{Tidal}}(f)$. We consider the amplitude formula up to the 3PN order as summarized in Ref. [69], where the point particle and the spin effects are included for both BBH and ECO hypotheses and the leading-order term is approximately written as approximately $\sim d_L^{-1}(\mathcal{M}^{\text{det}})^{5/6}f^{-7/6}$ where d_L is the luminosity distance to the source and $\mathcal{M}^{\text{det}} = (1+z)(m_1m_2)^{3/5}/(m_1+m_2)^{1/5}$ is the detector-frame (redshifted) chirp mass, which gives the leading-order evolution of the binary amplitude and phase, and z is the source redshift.

We use an extended model of TaylorF2 [42, 44, 45], TF2g, as $\Psi_{\text{BBH}}(f)$, which consists of point-particle and

spin parts. For TaylorF2 the 3.5PN-order formula is employed for the point-particle part of the phase as summarized in Refs. [45, 69]. For TF2g, the phase of the point-particle part is extended to the quasi 5.5PN order, which is derived by the Taylor expansion of the effective-one-body formula taking into account the notion in the test particle limit [46]. We set the uncalculated terms at 4PN order and beyond to zero. The added higher PN-order terms enable us to reduce the tidal deformability biasing.

The waveform models for both BBH and binary ECO used in our parameter estimation analyses assume that the spins of component objects are aligned with the orbital angular momentum and incorporate the 3.5PN-order formula in couplings between the orbital angular momentum and the component spins [70], 3PN-order formula in point-mass spin-spin, and self-spin interactions [71, 72] as summarized in Ref. [69]. The different PN-order terms for spin effects could help to break degeneracy between parameters.

We also use the PN formula for the tidal effects. We employ the 2.5PN-order (relative 5+2.5PN-order) tidal part of the phase. Recently, Henry *et al.* [73] have derived the complete form up to 5+2.5PN order for the mass quadrupole, current quadrupole, and mass octupole contributing to the GW tidal phase. We rewrite it only for the mass quadrupole interactions as a function of the dimensionless tidal deformability of each object defined as $\Lambda_{1,2} = \lambda_{1,2}/m_{1,2}^5$ by²

$$\begin{aligned} \Psi_{\text{Tidal}}(f) = & \frac{3}{128\eta}x^{5/2} \sum_{A=1}^2 \Lambda_A X_A^4 \left[-24(12 - 11X_A) - \frac{5}{28}(3179 - 919X_A - 2286X_A^2 + 260X_A^3)x \right. \\ & + 24\pi(12 - 11X_A)x^{3/2} \\ & - 5 \left(\frac{193986935}{571536} - \frac{14415613}{381024}X_A - \frac{57859}{378}X_A^2 - \frac{209495}{1512}X_A^3 + \frac{965}{54}X_A^4 - 4X_A^5 \right) x^2 \\ & \left. + \frac{\pi}{28}(27719 - 22415X_A + 7598X_A^2 - 10520X_A^3)x^{5/2} \right], \end{aligned} \quad (4)$$

where $x = [\pi M_{\text{tot}}(1+z)f]^{2/3}$ is the dimensionless PN expansion parameter, $M_{\text{tot}} = m_1 + m_2$ is the total mass, $\eta = m_1m_2/(m_1+m_2)^2$ is the symmetric mass ratio, and $X_A = m_A/M_{\text{tot}}$, $A=1,2$. Here, we do not ignore the anti-symmetric contribution $\delta\tilde{\Lambda}$ terms, while they are always subdominant on the tidal effects to the GW phase, compared with the symmetric contribution $\tilde{\Lambda}$ terms [48, 49]. We have implemented the complete GW tidal phase up to 5+2.5 PN-order and the tidal amplitude up to 5+1

PN-order for the mass quadrupole interactions and used it in our analyses.

The leading-order effect due to the SIQM appears as a part of spin-spin interactions in the PN phase at relative 2PN order [10], and the leading-order additional term for binary ECO is described as

$$\Psi_{\text{SIQM}}(f) = \frac{75}{64} \frac{\delta\kappa_1 m_1^2 \chi_1^2 + \delta\kappa_2 m_2^2 \chi_2^2}{m_1 m_2} x^{-1/2}. \quad (5)$$

In our analysis, we also incorporate relative 3PN corrections to the GW phase due to the SIQM effects as described in Refs. [33, 71, 74]. The expression for the SIQM parts in terms of $\delta\kappa_s$ and $\delta\kappa_a$ are described in Ref. [33], in which $\delta\kappa_a$ are the antisymmetric combination of the

² We will extend the our analysis by adding the current quadrupole and mass octupole interactions.

component SIQMs defined as $\delta\kappa_a = (\delta\kappa_1 - \delta\kappa_2)/2$.

In summary, our template models are the `TF2g`, `TF2g.Tidal`, `TF2g.SIQM`, and `TF2g.Tidal.SIQM` waveform models, which are, respectively, the reference BBH model, the ones with only the tidal terms, the ones with only the SIQM terms, and the ones with both the tidal and the SIQM terms.

C. Bayesian inference

We employ Bayesian inference for GW parameter estimation and model selection (see Refs. [75, 76] for review) between binary ECO and BBH. Given data d , which contains the signal and the noise, according to Bayes's theorem, the posterior distribution of the signal parameters θ that the waveform $\tilde{h}(\theta)$ depends on is given by

$$p(\theta|d) = \frac{\mathcal{L}(d|\theta)\pi(\theta)}{\mathcal{Z}}, \quad (6)$$

where $\mathcal{L}(d|\theta)$ is the likelihood function of the data for given parameters θ , $\pi(\theta)$ is the prior distribution for θ , and \mathcal{Z} is the evidence. By assuming stationarity and Gaussianity for the detector noise, the likelihood function is evaluated as,

$$\mathcal{L}(d|\theta) \propto \exp\left[-\frac{\langle d - h(\theta) | d - h(\theta) \rangle}{2}\right], \quad (7)$$

where the noise-weighted inner product $\langle \cdot | \cdot \rangle$ is defined by

$$\langle a | b \rangle := 4\text{Re} \int_{f_{\text{low}}}^{f_{\text{high}}} df \frac{\tilde{a}^*(f)\tilde{b}(f)}{S_n(f)}, \quad (8)$$

using the noise power spectrum density $S_n(f)$. We use $S_n(f)$ obtained with the `BayesLine` algorithm [77–79]. The lower limit of the integration f_{low} is the seismic cutoff frequency and the higher limit f_{high} is the cutoff frequency of waveforms. To restrict the analysis to the inspiral regimes of the signals, we set the upper frequency cutoff f_{high} to be referred to the one used in Refs. [3, 80].

The evidence is obtained as the likelihood marginalized over the prior volume,

$$\mathcal{Z} = \int d\theta \mathcal{L}(d|\theta)\pi(\theta). \quad (9)$$

To perform model selection between the binary ECO and BBH hypotheses, we compute the ratio between two different evidences, called the Bayes factor,

$$\text{BF}_{\text{BBH}}^{\text{ECO}} = \frac{\mathcal{Z}_{\text{ECO}}}{\mathcal{Z}_{\text{BBH}}}. \quad (10)$$

The combined Bayes factor is defined as

$$\log_{10} \text{BF}_{\text{BBH, total}}^{\text{ECO}} = \sum_i \log_{10} \text{BF}_{\text{BBH, i}}^{\text{ECO}}, \quad (11)$$

where $\text{BF}_{\text{BBH, i}}^{\text{ECO}}$ is the Bayes factor for individual events. The one-dimensional posterior for a specific parameter is

obtained by marginalizing the multidimensional posterior over the other parameters.

We compute posterior probability distribution functions (PDFs) by using Bayesian stochastic sampling based on the nested sampling algorithm [81, 82]. Specifically, we use the parameter estimation software, LAL-Inference [76], which is one of the software programs of LIGO Algorithm Library (LAL) software suite [83]. We select low-mass mergers in GWTC-2 [2] which have higher frequency cutoff ($f_{\text{high}} \gtrsim 120$ Hz) and larger inspiral signal-to-noise ratios (SNRs) ($\rho_{\text{inspiral}} \gtrsim 9$) (see Table V in the paper on tests of GR by the LVC [3]). We take the low-frequency cutoff $f_{\text{low}} = 20$ Hz for all events but 30 Hz for Hanford data for GW170608 by following the papers which reported the detection [84] and the high-frequency cutoff $f_{\text{high}} = 150$ Hz for GW151226, $f_{\text{high}} = 180$ Hz for GW170608, $f_{\text{high}} = 160$ Hz for GW190707, $f_{\text{high}} = 125$ Hz for GW190720, $f_{\text{high}} = 160$ Hz for GW190728, and $f_{\text{high}} = 175$ Hz for GW190924, which are determined to be restricted to the inspiral regime.

D. Source parameters and their priors

The source parameters and their prior probability distributions are basically chosen to follow those adopted in the paper on GWTC-2 by the LVC [2] and our recent work for GW analysis of BNSs [16, 17]. We mention the specific choices adopted below.

For BBH hypothesis, the parameters are the component masses $m_{1,2}$, where we assume $m_1 \geq m_2$; the orbit-aligned dimensionless spin components of the objects $\chi_{1,2}$; the luminosity distance to the source d_L ; the binary inclination angle θ_{JN} , which is the angle between the total angular momentum and the line of sight; the polarization angle ψ ; the coalescence time t_c ; and the phase at the coalescence time ϕ_c . For binary ECO hypothesis, we add the binary tidal deformability $\tilde{\Lambda}$, and the SIQMs $\delta\kappa_{1,2}$.

We employ a uniform prior on the detector-frame component masses $m_{1,2}^{\text{det}}$ in the range $[1.0, 60.0]M_{\odot}$. We assume a uniform prior on the spin magnitudes $\chi_{1,2}$ in the range $[-0.99, 0.99]$. We assume a uniform prior on both the binary tidal deformability $\tilde{\Lambda}$ and the asymmetric contribution $\delta\tilde{\Lambda}$ in the range $[-3000, 3000]$ and a uniform prior on the SIQMs for individual objects $\delta\kappa_{1,2}$ in the range $[-200, 200]$. While in the analysis of the paper on tests of GR by the LVC, they restrict $\delta\kappa_a = (\delta\kappa_1 - \delta\kappa_2)/2 = 0$, implying $\delta\kappa_1 = \delta\kappa_2 = \delta\kappa_s$ [3], we do not assume so.

III. RESULTS

We analyze the BBH events with the low-mass (or long inspiral regime) and higher SNR for the inspiral regime among GWTC-2 events [2, 85]. Here, we use

the public data on the Gravitational Wave Open Science Center (<https://www.gw-openscience.org>) released by the LVC. We analyze each event using inspiral-only template TF2g_Tidal_SIQM waveform model. First, we present the results for the largest SNR event GW170608 in detail. Next, we show the results for other events and model selection by the Bayes factor combining six events.

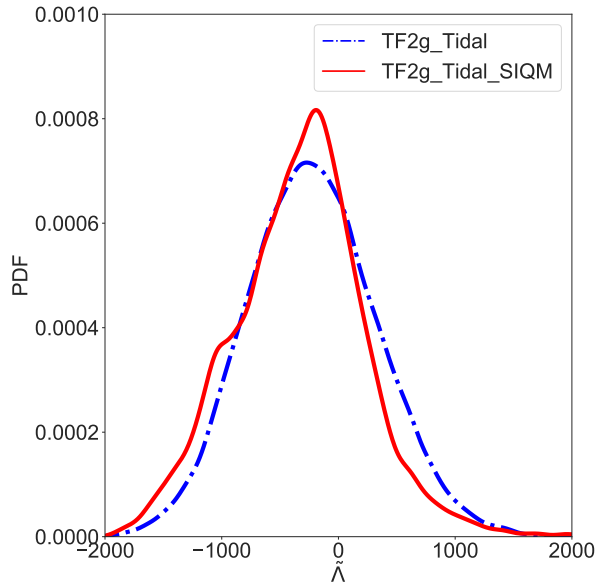


FIG. 1. Marginalized posterior PDFs of $\tilde{\Lambda}$ for low-mass event GW170608 with the TF2g_Tidal (blue, dashed) and TF2g_Tidal_SIQM (red, solid) waveform models. We set $f_{\text{high}} = 180$ Hz. Adding the SIQM terms do not affect the constraint on the tidal deformability $\tilde{\Lambda}$.

TABLE I. The logarithm of the Bayes factors for a signal compared to Gaussian noise $\log_{10} \text{BF}_{s/n}$ and SNRs for GW170608 using the TF2g, TF2g_Tidal, TF2g_SIQM, and TF2g_Tidal_SIQM waveform models. The tidal and SIQM terms do not affect the Bayes factor and SNR.

	$\log_{10} \text{BF}_{s/n}$	SNR
TF2g (BBH in GR)	71.3	14.7
TF2g_Tidal	69.8	14.7
TF2g_SIQM	70.4	14.7
TF2g_Tidal_SIQM	69.3	14.7

A. Estimating tidal deformability and SIQMs for GW170608

We show the results of low-mass presumed BBH event GW170608. We present posteriors of binary tidal deformability and the SIQM for GW170608. Figure 1 shows posteriors of $\tilde{\Lambda}$ for GW170608. We set $f_{\text{high}} = 180$ Hz.

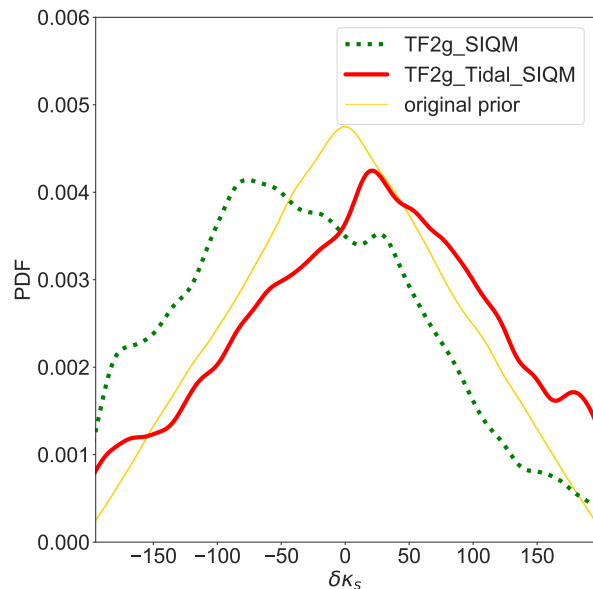


FIG. 2. Marginalized posterior PDFs of $\delta\kappa_s$ for GW170608 using the TF2g_SIQM (green, dotted) and TF2g_Tidal_SIQM (red, solid) waveform models. We set $f_{\text{high}} = 180$ Hz. They are weighted by dividing the original prior: uniform on $\delta\kappa_{1,2}$. The original prior is also shown by solid yellow curve. The peak of $\delta\kappa_s$ is shifted toward zero by adding the tidal terms.

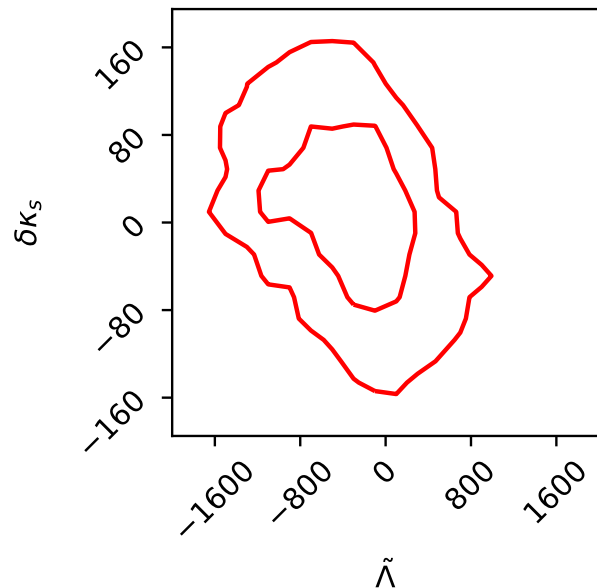


FIG. 3. Corner plot on the $\tilde{\Lambda}$ - $\delta\kappa_s$ plane for GW170608 using the TF2g_Tidal_SIQM waveform model by setting $f_{\text{high}} = 180$ Hz. The contours correspond to 50% and 90% credible regions. The constraints show that GW170608 are consistent with BBH in GR ($\tilde{\Lambda} = \delta\kappa_s = 0$).

The posterior distribution of $\tilde{\Lambda}$ for the TF2g_Tidal waveform model (blue dot-dashed) is consistent with the one for the TF2g_Tidal_SIQM waveform model (red solid). Adding the SIQM terms does not affect the constraint on the tidal deformability $\tilde{\Lambda}$.

Figure 2 shows posteriors of $\delta\kappa_s$ for GW170608 using the TF2g_SIQM and TF2g_Tidal_SIQM waveform models. Here, they are weighted by dividing the original prior, uniform on $\delta\kappa_{1,2}$, to effectively impose a uniform prior on $\delta\kappa_s$. We find that $\delta\kappa_s$ is poorly constrained for GW170608 for both templates, which is consistent with the results shown for the templates with only the SIQMs in Refs. [3, 36]. Equation (2) shows that $Q_i = 0$ when $\chi_i = 0$, independent of the value of $\delta\kappa_i$, and $\delta\kappa_i$ is not constrained unless at least one of the magnitude of the component spin χ_i exclude zero. It is natural that our constraints on $\delta\kappa_s$ are poorer than LVC's since we do not assume $\delta\kappa_a = 0$. Comparing the posteriors for the TF2g_SIQM (green, dotted) with TF2g_Tidal_SIQM (red, solid) waveform models, adding the tidal terms shifts the peak of $\delta\kappa_s$ toward zero.

Figure 3 shows the corner plot on the $\tilde{\Lambda}$ - $\delta\kappa_s$ plane for GW170608 using the TF2g_Tidal_SIQM waveform model, which shows that the observed data are consistent with BBH in GR ($\tilde{\Lambda} = \delta\kappa_s = 0$). This figure shows the posterior of $\delta\kappa_s$ for the uniform prior on $\delta\kappa_{1,2}$. We find a weak negative correlation between $\tilde{\Lambda}$ and $\delta\kappa_s$.

Table I shows the logarithm of the Bayes factor for a signal compared to Gaussian noise $\log_{10} \text{BF}_{s/n}$. Adding the tidal and SIQM terms does not drastically change the Bayes factor $\log_{10} \text{BF}_{s/n}$ and SNRs.

B. Biases of binary parameters due to tidal and SIQM terms for GW170608

Figure 4 shows the marginalized posterior PDFs of parameters other than the tidal deformability and the SIQM obtained by using the TF2g model (orange, solid), TF2g_Tidal (blue, dot-dashed), TF2g_SIQM (green, dotted), and TF2g_Tidal_SIQM (red, dashed) waveform models. We present the distribution of the mass parameters: the mass ratio $q = m_2/m_1$, the primary mass m_1 , the secondary mass m_2 , the chirp mass \mathcal{M} , the detector-frame chirp mass \mathcal{M}^{det} and the total mass M_{tot} , the luminosity distance d_L , the binary inclination θ_{JN} , and the effective inspiral spin χ_{eff} , which gives the leading-order spin effect on the binary phase evolution [86, 87] defined as $\chi_{\text{eff}} = (m_1\chi_1 + m_2\chi_2)/M_{\text{tot}}$. The source-frame chirp mass is derived by assuming the Hubble constant $H_0 = 69 \text{ km s}^{-1} \text{ Mpc}^{-1}$ (a default value in LALInference adopted from Planck 2013 results [88]). q , m_1 , m_2 , \mathcal{M} , M_{tot} , d_L , and θ_{JN} are not affected by adding the tidal and SIQM terms to the TF2g baseline model. Adding either the tidal or the SIQM terms shifts the peak of χ_{eff} toward zero, as also shown in Fig. 5 of Ref. [36] for SIQM, which is because measurement of χ_{eff} becomes difficult. This also biases the estimate of \mathcal{M}^{det} . Comparing the poste-

riors of χ_{eff} for the TF2g_Tidal (blue dot-dashed) with TF2g_Tidal_SIQM (red solid) waveform models, adding the SIQM terms reduces the statistical error of χ_{eff} .

C. Constraints on tidal deformability and SIQMs for GWTC-2 events

We also analyzed other five low-mass events: GW151226 with $f_{\text{high}} = 150 \text{ Hz}$, GW190707 with $f_{\text{high}} = 160 \text{ Hz}$, GW190720 with $f_{\text{high}} = 125 \text{ Hz}$, GW190728 with $f_{\text{high}} = 160 \text{ Hz}$, and GW190924 with $f_{\text{high}} = 175 \text{ Hz}$, using the TF2g_Tidal_SIQM waveform model. We present posteriors of binary tidal deformability and the SIQMs for GW151226, GW170608, GW190707, GW190720, GW190728, and GW190924. The left panel of Fig. 5 shows posteriors of $\tilde{\Lambda}$ for six events using the TF2g_Tidal_SIQM waveform model. This figure shows the posterior of $\delta\kappa_s$ for the uniform prior on $\delta\kappa_{1,2}$. The 90% symmetric credible ranges of $\tilde{\Lambda}$ are summarized in Table II, which are $[-1441, 649]$ for GW151226, $[-1265, 565]$ for GW170608, $[-1265, 565]$ for GW170608, $[-590, 1661]$ for GW190707, $[-1445, 1768]$ for GW190720, $[-1432, 1078]$ for GW190728, and $[-2041, 1118]$ for GW190924.

The right panel of Fig. 5 shows the posterior distribution on the $\tilde{\Lambda}$ - $\delta\kappa_s$ plane. For all events, there exists negative correlation between $\tilde{\Lambda}$ and $\delta\kappa_s$. We find that $\delta\kappa_s$ is poorly constrained for all events we analyzed, which is consistent with the results in Refs. [3, 36]. We do not show the credible intervals for $\delta\kappa_s$, since all the posterior PDFs present tails reaching the edge of the prior when they are divided by the original prior (uniform on $\delta\kappa_{1,2}$) as shown in Fig. 2 for GW170608 and in Refs. [3, 36] for other cases. It is natural that our constraints on $\delta\kappa_s$ are poorer than LVC's, since we do not assume $\delta\kappa_a = 0$, while LVC did.

D. Model selection between ECO and BBH

The Bayes factor between the binary ECO and BBH waveform model, $\text{BF}_{\text{BBH}}^{\text{ECO}}$, quantifies the statistical significance of one hypothesis over the other. The binary ECO hypothesis (the TF2g_Tidal_SIQM waveform model) is disfavored compared to BBH (the TF2g waveform model) for all events as shown Table II³.

The combined Bayes factor of six events estimated by using Eq. (11), $\log_{10} \text{BF}_{\text{BBH, total}}^{\text{ECO}} = -10.4$, shows that the BBH hypothesis is preferred to the binary ECO hypothesis.

³ $\log_{10} \text{BF} > 1.5$ is often interpreted as a strong preference for one model over another, and $\log_{10} \text{BF} > 2$ is interpreted as decisive evidence [89].

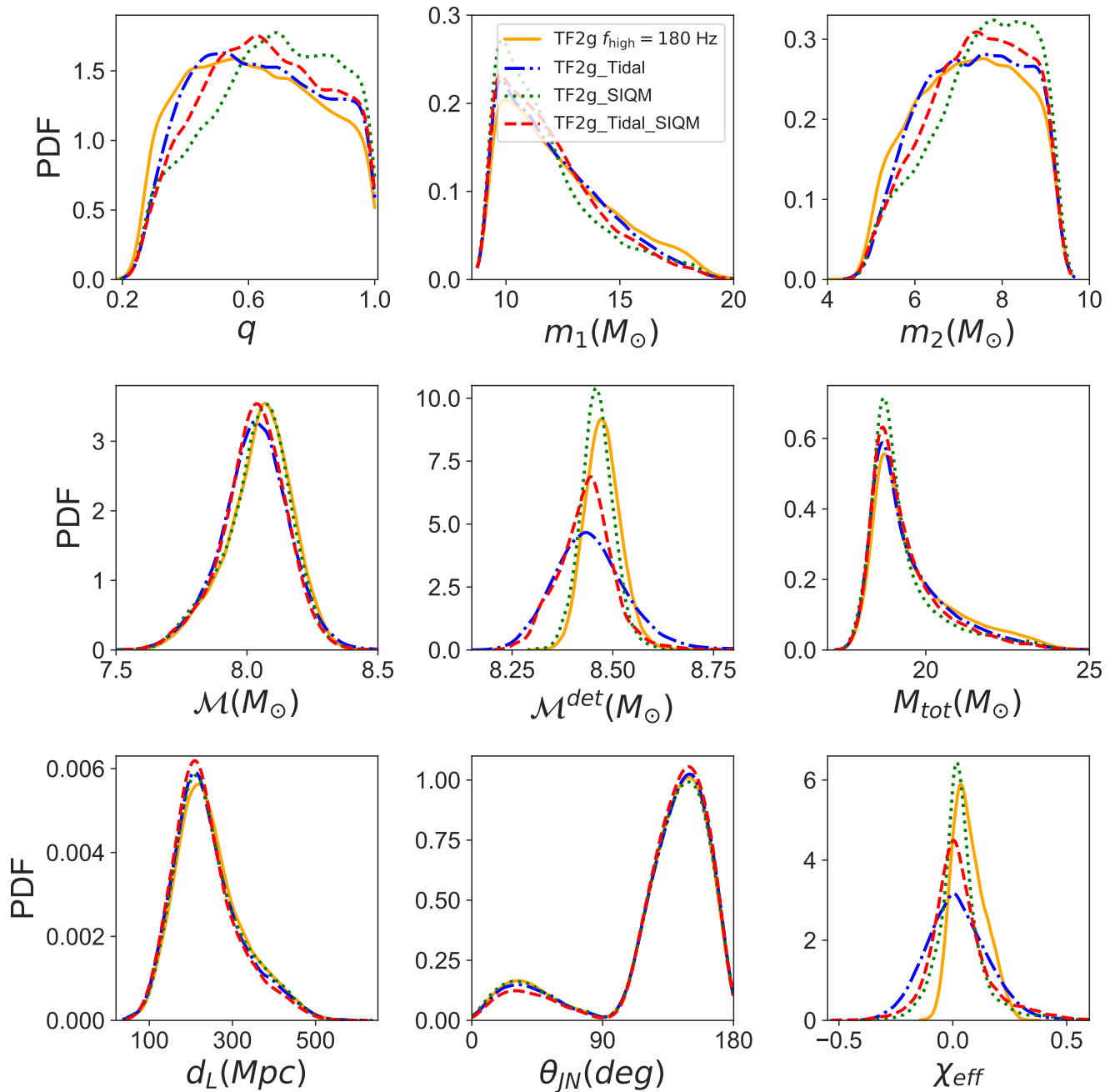


FIG. 4. Marginalized posterior PDFs of various parameters for GW170608 derived by using the TF2g (orange, solid), TF2g_Tidal (blue, dot-dashed), TF2g_SIQM (green, dotted), and TF2g_Tidal_SIQM (red, dashed) waveform models, by setting $f_{\text{high}} = 180$ Hz. The top-left, top-middle, top-right, middle-left, center, middle-right, bottom-left, bottom-middle, and bottom-right panels show the mass ratio q , the primary mass m_1 , the secondary mass m_2 , the source-frame chirp mass \mathcal{M} , the detector-frame chirp mass \mathcal{M}^{det} , the total mass M_{tot} , the luminosity distance to the source d_L , the inclination angle θ_{JN} , and the effective spin parameter χ_{eff} , respectively. Adding either the tidal or the SIQM terms shifts the peak of χ_{eff} toward zero, due to the difficulty of measuring χ_{eff} .

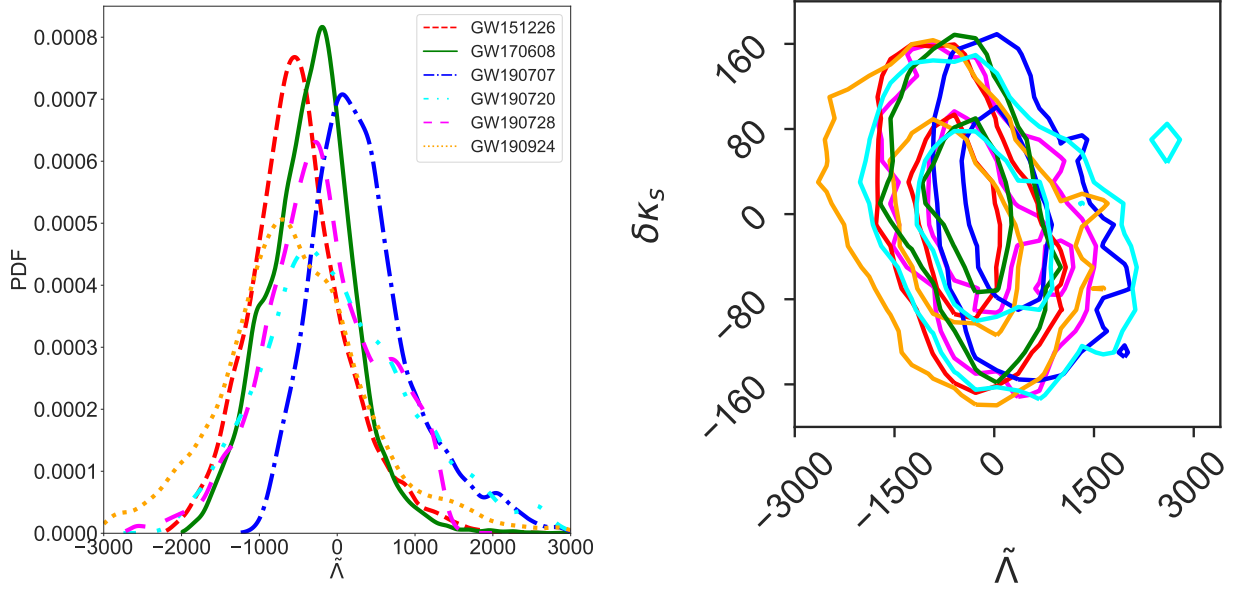


FIG. 5. Left: the same as Fig. 1 but for GW151226 (red dashed), GW170608 (green solid), GW190707 (blue dot-dashed), GW190720 (cyan dash-dot-dotted), GW190728 (magenta loosely dashed), and GW190924 (orange dotted), using the `TF2g-Tidal-SIQM` waveform model by setting $f_{\text{high}} = 150, 180, 160, 125, 160,$ and 175 Hz, respectively. These constraints show that all events are consistent with BBH in GR ($\tilde{\Lambda} = 0$). Right: the same as Fig. 3 but for GW151226 (red), GW170608 (green), GW190707 (blue), GW190720 (cyan), GW190728 (magenta), and GW190924 (orange) using the `TF2g-Tidal-SIQM` waveform model for $f_{\text{high}} = 150, 180, 160, 125, 160,$ and 175 Hz, respectively. These constraints show that all events are consistent with BBH in GR ($\tilde{\Lambda} = \delta\kappa_s = 0$).

TABLE II. The 90% symmetric credible ranges of $\tilde{\Lambda}$, the logarithm of the Bayes factors between binary ECO and BBH, i.e., $\log_{10} \text{BF}_{\text{BBH}}^{\text{ECO}}$, and SNRs for GW151226, GW170608, GW190707, GW190720, GW190728, GW190924, and the result combining six events using the TF2g_Tidal_SIQM waveform model with respective f_{high} . For individual events, $\log_{10} \text{BF}_{\text{BBH}}^{\text{ECO}}$ are negative, thus favoring the BBH in GR compared to binary ECO. For the combined case, $\log_{10} \text{BF}_{\text{BBH, total}}^{\text{ECO}}$ is also negative, thus disfavoring the binary ECO.

Event	f_{high} (Hz)	$\tilde{\Lambda}$	$\log_{10} \text{BF}_{\text{BBH}}^{\text{ECO}}$	SNR
GW151226	150	[-1441, 649]	-0.45	10.7
GW170608	180	[-1265, 565]	-2.1	14.7
GW190707	160	[-590, 1661]	-2.1	11.2
GW190720	125	[-1445, 1768]	-1.8	9.3
GW190728	160	[-1432, 1078]	-2.0	12.1
GW190924	175	[-2041, 1118]	-2.0	11.4
Combined	-	-	-10.4	-

IV. CONCLUSION

We implemented the tidal and SIQM terms in the aligned-spin PN inspiral waveform model TF2g, which we call TF2g_Tidal_SIQM. We analyzed six low-mass events GW151226, GW170608, GW190707, GW190720, GW190728, and GW190924 using the TF2g_Tidal_SIQM waveform model as templates. The obtained results are the first constraints on the tidal deformability of the events classified as BBH in GWTC-2 events, motivated by ECO hypotheses. We found that all events that we have analyzed are consistent with BBH mergers in GR. The logarithmic Bayes factor $\log_{10} \text{BF}_{\text{BBH}}^{\text{ECO}}$ for individual events is less than -1.5 except for GW151226, thus favoring the BBH in GR compared to binary ECO by Bayesian model selection. The combined logarithmic Bayes factor between the binary ECO and BBH is $\log_{10} \text{BF}_{\text{BBH, total}}^{\text{ECO}} = -10.1$, which means that the ECO or non-GR model (with Tidal and SIQM parameters) is also disfavored compared to BBH in GR.

In this paper, we used the inspiral-only waveform model as templates because there is no robust prediction waveform of the merger-ringdown regimes of the binary ECO merger. It might be interesting to use a toy model for postcontact regimes of binary ECOs, which has been recently derived [31]. Also, GW echoes could be used to examine postmerger regime. Such extensions including the waveform after the inspiral regime would allow us to analyze heavy-mass events and to put a different type of constraints on ECO hypothesis.

ACKNOWLEDGMENT

T. Narikawa thanks Chris van den Broeck and Anuradha Samajdar for useful discussions, and he is also

thankful for the hospitality of the Chris's group, in particular Khun Sang Phukon, Archisman Gosh, and Tim Dietrich, during his stay at Nikhef. We thank Aditya Vijaykumar, Nathan K. Johnson-McDaniel, Rahul Kashyap, Arunava Mukherjee, and Parameswaran Ajith for sharing and discussing their results on a similar study [91]. We would like to thank Soichiro Morisaki, Kyohei Kawaguchi, and Hideyuki Tagoshi for fruitful discussions. We thank Quentin Henry and Luc Blanchet for pointing out the complete GW tidal phase they have derived and confirming the correction that the expression that we have rewritten with their value for the mass quadrupole part as a function of $\Lambda_{1,2}$, especially the 2 and 2.5 PN-order terms. T. Narikawa was supported in part by a Grant-in-Aid for JSPS Research Fellows. This work is supported by Japanese Society for the Promotion of Science (JSPS) KAKENHI Grants No. JP21K03548, No. JP17H06361, No. JP17H06358, No. JP17H06357, and No. JP20K03928. We would also like to thank Computing Infrastructure ORION in Osaka City University. We are also grateful to the LIGO-Virgo Collaboration for the public release of gravitational-wave data of GW151226, GW170608, GW190707_093326, and GW190924.021846. This research has made use of data, software, and web tools obtained from the Gravitational Wave Open Science Center (<https://www.gwopenscience.org>), a service of LIGO Laboratory, the LIGO Scientific Collaboration and the Virgo Collaboration. LIGO is funded by the U. S. National Science Foundation. Virgo is funded by the French Centre National de la Recherche Scientifique (CNRS), the Italian Istituto Nazionale di Fisica Nucleare (INFN), and the Dutch Nikhef, with contributions by Polish and Hungarian institutes.

Appendix A: Results by using TF2 waveform model

While we show the results by using the TF2g_Tidal_SIQM waveform model in Sec. III, we show the results for seven events added GW190814 by using the TF2_Tidal_SIQM waveform model in this Appendix. For highly unequal mass ratio events GW190814, the TF2g waveform model does not work well due to setting the uncalculated terms at high PN order to zero. We take the low-frequency cutoff $f_{\text{low}} = 20$ Hz for Hanford data and 30 Hz for Livingston data for GW190814 by following the papers which reported the detection [90] and the high-frequency cutoff $f_{\text{high}} = 140$ Hz.

We present posteriors of binary tidal deformability and the SIQMs for GW151226, GW170608, GW190707, GW190720, GW190728, GW190814 and GW190924 by using the TF2_Tidal_SIQM waveform model.

The left panel of Fig. 6 shows posteriors of $\tilde{\Lambda}$ for seven events using the TF2_Tidal_SIQM waveform model. The right panel of Fig. 6 shows the posterior distribution on $\tilde{\Lambda}$ - $\delta\kappa_{\tilde{s}}$ plane. The 90% symmetric credible ranges of $\tilde{\Lambda}$ are summarized in

Table III, which are $[-1656, 590]$ for GW151226, $[-1299, 520]$ for GW170608, $[-791, 1487]$ for GW190707, $[-1523, 1436]$ for GW190720, $[-1445, 846]$ for GW190728, $[-786, 1272]$ for GW190814, and $[-2093, 939]$ for GW190924. Except for GW190814, systematic uncertainty between TF2g_Tidal_SIQM and TF2_Tidal_SIQM results remains subdominant to statistical uncertainty.

We show the Bayes factor between the binary ECO and BBH waveform model, $\text{BF}_{\text{BBH}}^{\text{ECO}}$ in Table III. The binary ECO hypothesis (the TF2_Tidal_SIQM waveform model) is disfavored compared to BBH (the TF2g waveform model) for all events. The combined Bayes factor of seven events are $\log_{10} \text{BF}_{\text{BBH, total}}^{\text{ECO}} = -14.0$ shows that BBH hypothesis is preferred to the binary ECO hypothesis as shown for TF2g_Tidal_SIQM.

TABLE III. The same as Table II but for the TF2_Tidal_SIQM waveform model and GW190814 is added. For both the individual events and the combined case, the log Bayes factor $\log_{10} \text{BF}_{\text{BBH, total}}^{\text{ECO}}$ is negative, thus disfavoring binary ECO.

Event	f_{high} (Hz)	$\hat{\Lambda}$	$\log_{10} \text{BF}_{\text{BBH}}^{\text{ECO}}$	SNR
GW151226	150	$[-1656, 590]$	-0.66	10.7
GW170608	180	$[-1299, 520]$	-1.8	14.7
GW190707	160	$[-791, 1487]$	-2.0	11.2
GW190720	125	$[-1523, 1436]$	-1.3	9.3
GW190728	160	$[-1445, 846]$	-1.9	12.1
GW190814	140	$[-786, 1272]$	-4.0	22.0
GW190924	175	$[-2093, 939]$	-2.2	11.4
Combined	-	-	-14.0	-

- [1] B. P. Abbott *et al.* [LIGO Scientific and Virgo], “GWTC-1: A Gravitational-Wave Transient Catalog of Compact Binary Mergers Observed by LIGO and Virgo during the First and Second Observing Runs,” *Phys. Rev. X* **9**, 031040 (2019) [arXiv:1811.12907 [astro-ph.HE]].
- [2] R. Abbott *et al.* [LIGO Scientific and Virgo], “GWTC-2: Compact Binary Coalescences Observed by LIGO and Virgo During the First Half of the Third Observing Run,” [arXiv:2010.14527 [gr-qc]].
- [3] R. Abbott *et al.* [LIGO Scientific and Virgo], “Tests of General Relativity with Binary Black Holes from the second LIGO-Virgo Gravitational-Wave Transient Catalog,” [arXiv:2010.14529 [gr-qc]].
- [4] V. Cardoso and P. Pani, “Testing the nature of dark compact objects: a status report,” *Living Rev. Rel.* **22**, 4 (2019) [arXiv:1904.05363 [gr-qc]].
- [5] E. Poisson and C. Will, “Gravity: Newtonian, Post-Newtonian, Relativistic” (Cambridge University Press, Cambridge, England, 2014).
- [6] E. E. Flanagan and T. Hinderer, “Constraining neutron star tidal Love numbers with gravitational wave detectors,” *Phys. Rev. D* **77**, 021502 (2008) [arXiv:0709.1915 [astro-ph]].
- [7] T. Hinderer, “Tidal Love numbers of neutron stars,” *Astrophys. J.* **677**, 1216 (2008) [arXiv:0711.2420 [astro-ph]].
- [8] T. Damour, A. Nagar and L. Villain, “Measurability of the tidal polarizability of neutron stars in late-inspiral gravitational-wave signals”, *Phys. Rev. D* **85**, 123007 (2012) [arXiv:1203.4352 [gr-qc]].
- [9] M. Agathos, J. Meidam, W. Del Pozzo, T. G. F. Li, M. Tompitak, J. Veitch, S. Vitale and C. Van Den Broeck, “Constraining the neutron star equation of state with gravitational wave signals from coalescing binary neutron stars,” *Phys. Rev. D* **92**, no.2, 023012 (2015) [arXiv:1503.05405 [gr-qc]].
- [10] E. Poisson, “Gravitational waves from inspiraling compact binaries: The Quadrupole moment term,” *Phys. Rev. D* **57**, 5287-5290 (1998) [arXiv:gr-qc/9709032 [gr-qc]].
- [11] K. Yagi and N. Yunes, “I-Love-Q,” *Science* **341**, 365-368 (2013) [arXiv:1302.4499 [gr-qc]].
- [12] K. Yagi and N. Yunes, “I-Love-Q Relations in Neutron Stars and their Applications to Astrophysics, Gravitational Waves and Fundamental Physics,” *Phys. Rev. D* **88**, 023009 (2013) [arXiv:1303.1528 [gr-qc]].
- [13] B. P. Abbott *et al.* [LIGO Scientific and Virgo Collaborations], “Properties of the binary neutron star merger GW170817,” *Phys. Rev. X* **9**, 011001 (2019) [arXiv:1805.11579 [gr-qc]].
- [14] B. P. Abbott *et al.* [LIGO Scientific and Virgo], “GW170817: Measurements of neutron star radii and equation of state,” *Phys. Rev. Lett.* **121**, 161101 (2018) [arXiv:1805.11581 [gr-qc]].
- [15] B. P. Abbott *et al.* [LIGO Scientific and Virgo], “GW190425: Observation of a Compact Binary Coalescence with Total Mass $\sim 3.4M_{\odot}$,” *Astrophys. J. Lett.* **892**, L3 (2020) [arXiv:2001.01761 [astro-ph.HE]].
- [16] T. Narikawa, N. Uchikata, K. Kawaguchi, K. Kiuchi, K. Kyutoku, M. Shibata and H. Tagoshi, “Discrepancy in tidal deformability of GW170817 between the Advanced LIGO twin detectors,” *Phys. Rev. Research.* **1**, 033055 (2019) [arXiv:1812.06100 [astro-ph.HE]].
- [17] T. Narikawa, N. Uchikata, K. Kawaguchi, K. Kiuchi, K. Kyutoku, M. Shibata and H. Tagoshi, “Reanalysis of the binary neutron star mergers GW170817 and GW190425 using numerical-relativity calibrated waveform models,” *Phys. Rev. Res.* **2**, 043039 (2020) [arXiv:1910.08971 [gr-qc]].
- [18] J. B. Hartle, “Tidal Friction in Slowly Rotating Black Holes,” *Phys. Rev. D* **8**, 1010-1024 (1973)
- [19] S. A. Hughes, “Evolution of circular, nonequatorial orbits of Kerr black holes due to gravitational wave emission. II. Inspiral trajectories and gravitational wave forms,” *Phys. Rev. D* **64**, 064004 (2001) [erratum: *Phys. Rev. D* **88**, 109902 (2013)] [arXiv:gr-qc/0104041 [gr-qc]].
- [20] A. Maselli, P. Pani, V. Cardoso, T. Abdelsalhin, L. Gualtieri and V. Ferrari, “Probing Planckian corrections at the horizon scale with LISA binaries,” *Phys. Rev. Lett.* **120**, 081101 (2018) [arXiv:1703.10612 [gr-qc]].
- [21] S. Isoyama and H. Nakano, “Post-Newtonian templates for binary black-hole inspirals: the effect of the horizon fluxes and the secular change in the black-hole

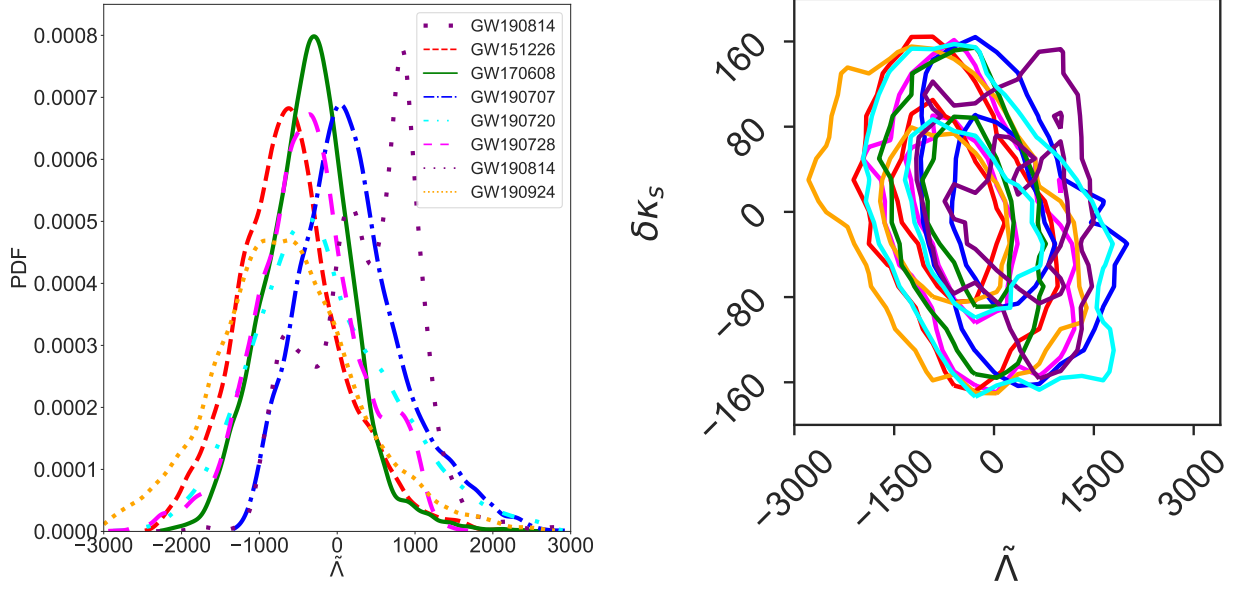


FIG. 6. Left: the same as the left panel of Fig. 5 but for the TF2_Tidal_SIQM waveform model and GW190814 (purple loosely dotted) is added. These constraints show that all events are consistent with BBH in GR ($\tilde{\Lambda} = 0$). Right: the same as the right panel of Fig. 5 but for the TF2_Tidal_SIQM waveform model and GW190814 (purple) is added. These constraints show that all events are consistent with BBH in GR ($\tilde{\Lambda} = \delta\kappa_s = 0$).

- masses and spins,” *Class. Quant. Grav.* **35**, 024001 (2018) [arXiv:1705.03869 [gr-qc]].
- [22] S. Datta, R. Brito, S. Bose, P. Pani and S. A. Hughes, “Tidal heating as a discriminator for horizons in extreme mass ratio inspirals,” *Phys. Rev. D* **101**, 044004 (2020) [arXiv:1910.07841 [gr-qc]].
- [23] S. Datta and S. Bose, “Probing the nature of central objects in extreme-mass-ratio inspirals with gravitational waves,” *Phys. Rev. D* **99**, 084001 (2019) [arXiv:1902.01723 [gr-qc]].
- [24] S. Datta, K. S. Phukon and S. Bose, “Recognizing black holes in gravitational-wave observations: Telling apart impostors in mass-gap binaries,” [arXiv:2004.05974 [gr-qc]].
- [25] N. Sago and T. Tanaka, “Oscillations in the EMRI gravitational wave phase correction as a probe of reflective boundary of the central black hole,” [arXiv:2106.07123 [gr-qc]].
- [26] K. Fransen, G. Koekoek, R. Tielemans and B. Vercocke, “Modeling and detecting resonant tides of exotic compact objects,” [arXiv:2005.12286 [gr-qc]].
- [27] Y. Asali, P. T. H. Pang, A. Samajdar and C. Van Den Broeck, “Probing resonant excitations in exotic compact objects via gravitational waves,” *Phys. Rev. D* **102**, 024016 (2020) [arXiv:2004.05128 [gr-qc]].
- [28] J. Abedi, H. Dykaar and N. Afshordi, “Echoes from the Abyss: Tentative evidence for Planck-scale structure at black hole horizons,” *Phys. Rev. D* **96**, 082004 (2017) [arXiv:1612.00266 [gr-qc]].
- [29] J. Westerweck, A. Nielsen, O. Fischer-Birnholtz, M. Cabero, C. Capano, T. Dent, B. Krishnan, G. Meadors and A. H. Nitz, “Low significance of evidence for black hole echoes in gravitational wave data,” *Phys. Rev. D* **97**, 124037 (2018) [arXiv:1712.09966 [gr-qc]].
- [30] N. Uchikata, H. Nakano, T. Narikawa, N. Sago, H. Tagoshi and T. Tanaka, “Searching for black hole echoes from the LIGO-Virgo Catalog GWTC-1,” *Phys. Rev. D* **100**, 062006 (2019) [arXiv:1906.00838 [gr-qc]].
- [31] A. Toubiana, S. Babak, E. Barausse and L. Lehner, “Modeling gravitational waves from exotic compact objects,” *Phys. Rev. D* **103**, 064042 (2021) [arXiv:2011.12122 [gr-qc]].
- [32] S. Kasta, A. Gupta, K. G. Arun, B. S. Sathyaprakash and C. Van Den Broeck, “Testing the multipole structure of compact binaries using gravitational wave observations,” *Phys. Rev. D* **98**, 124033 (2018) [arXiv:1809.10465 [gr-qc]].
- [33] N. V. Krishnendu, K. G. Arun and C. K. Mishra, “Testing the binary black hole nature of a compact binary coalescence,” *Phys. Rev. Lett.* **119**, 091101 (2017) [arXiv:1701.06318 [gr-qc]].
- [34] N. V. Krishnendu, C. K. Mishra and K. G. Arun, “Spin-induced deformations and tests of binary black hole nature using third-generation detectors,” *Phys. Rev. D* **99**, 064008 (2019) [arXiv:1811.00317 [gr-qc]].
- [35] N. V. Krishnendu and A. B. Yelikar, “Testing the Kerr nature of supermassive and intermediate-mass black hole binaries using spin-induced multipole moment measurements,” *Class. Quant. Grav.* **37**, 205019 (2020) [arXiv:1904.12712 [gr-qc]].
- [36] N. V. Krishnendu, M. Saleem, A. Samajdar, K. G. Arun, W. Del Pozzo and C. K. Mishra, “Constraints on the binary black hole nature of GW151226 and GW170608 from the measurement of spin-induced quadrupole moments,” *Phys. Rev. D* **100**, 104019 (2019) [arXiv:1908.02247 [gr-qc]].

- [37] M. Wade, J. D. E. Creighton, E. Ochsner and A. B. Nielsen, “Advanced LIGO’s ability to detect apparent violations of the cosmic censorship conjecture and the no-hair theorem through compact binary coalescence detections,” *Phys. Rev. D* **88**, 083002 (2013) [arXiv:1306.3901 [gr-qc]].
- [38] V. Cardoso, E. Franzin, A. Maselli, P. Pani and G. Raposo, “Testing strong-field gravity with tidal Love numbers,” *Phys. Rev. D* **95**, 084014 (2017) [arXiv:1701.01116 [gr-qc]].
- [39] N. Sennett, T. Hinderer, J. Steinhoff, A. Buonanno and S. Ossokine, “Distinguishing Boson Stars from Black Holes and Neutron Stars from Tidal Interactions in Inspiral Binary Systems,” *Phys. Rev. D* **96**, 024002 (2017) [arXiv:1704.08651 [gr-qc]].
- [40] N. K. Johnson-Mcdaniel, A. Mukherjee, R. Kashyap, P. Ajith, W. Del Pozzo and S. Vitale, “Constraining black hole mimickers with gravitational wave observations,” *Phys. Rev. D* **102**, 123010 (2020) [arXiv:1804.08026 [gr-qc]].
- [41] C. Pacilio, M. Vaglio, A. Maselli and P. Pani, “Gravitational-wave detectors as particle-physics laboratories: Constraining scalar interactions with a coherent inspiral model of boson-star binaries,” *Phys. Rev. D* **102**, 083002 (2020) [arXiv:2007.05264 [gr-qc]].
- [42] L. Blanchet, “Gravitational Radiation from Post-Newtonian Sources and Inspiral Compact Binaries,” *Living Rev. Rel.* **17**, 2 (2014) [arXiv:1310.1528 [gr-qc]].
- [43] S. Isoyama, R. Sturani and H. Nakano, “Post-Newtonian templates for gravitational waves from compact binary inspirals,” [arXiv:2012.01350 [gr-qc]].
- [44] S. V. Dhurandhar and B. S. Sathyaprakash, “Choice of filters for the detection of gravitational waves from coalescing binaries. 2. Detection in colored noise,” *Phys. Rev. D* **49**, 1707-1722 (1994)
- [45] A. Buonanno, B. Iyer, E. Ochsner, Y. Pan and B. S. Sathyaprakash, “Comparison of post-Newtonian templates for compact binary inspiral signals in gravitational-wave detectors”, *Phys. Rev. D* **80**, 084043 (2009) [arXiv:0907.0700 [gr-qc]].
- [46] F. Messina, R. Dudi, A. Nagar and S. Bernuzzi, “Quasi-5.5PN TaylorF2 approximant for compact binaries: point-mass phasing and impact on the tidal polarizability inference,” *Phys. Rev. D* **99**, 124051 (2019) [arXiv:1904.09558 [gr-qc]].
- [47] J. Vines, E. E. Flanagan and T. Hinderer, “Post-1-Newtonian tidal effects in the gravitational waveform from binary inspirals,” *Phys. Rev. D* **83**, 084051 (2011) [arXiv:1101.1673 [gr-qc]].
- [48] M. Favata, “Systematic parameter errors in inspiraling neutron star binaries,” *Phys. Rev. Lett.* **112**, 101101 (2014) [arXiv:1310.8288 [gr-qc]].
- [49] L. Wade, J. D. E. Creighton, E. Ochsner, B. D. Lackey, B. F. Farr, T. B. Littenberg and V. Raymond, “Systematic and statistical errors in a bayesian approach to the estimation of the neutron-star equation of state using advanced gravitational wave detectors”, *Phys. Rev. D* **89**, 103012 (2014) [arXiv:1402.5156 [gr-qc]].
- [50] T. Binnington and E. Poisson, “Relativistic theory of tidal Love numbers,” *Phys. Rev. D* **80**, 084018 (2009) [arXiv:0906.1366 [gr-qc]].
- [51] T. Damour and A. Nagar, “Effective One Body description of tidal effects in inspiralling compact binaries,” *Phys. Rev. D* **81**, 084016 (2010) [arXiv:0911.5041 [gr-qc]].
- [52] E. Poisson, “Tidal deformation of a slowly rotating black hole,” *Phys. Rev. D* **91**, no.4, 044004 (2015) [arXiv:1411.4711 [gr-qc]].
- [53] P. Pani, L. Gualtieri, A. Maselli and V. Ferrari, “Tidal deformations of a spinning compact object,” *Phys. Rev. D* **92**, 024010 (2015) [arXiv:1503.07365 [gr-qc]].
- [54] P. Landry and E. Poisson, “Tidal deformation of a slowly rotating material body. External metric,” *Phys. Rev. D* **91**, 104018 (2015) [arXiv:1503.07366 [gr-qc]].
- [55] T. Hinderer, B. D. Lackey, R. N. Lang and J. S. Read, “Tidal deformability of neutron stars with realistic equations of state and their gravitational wave signatures in binary inspiral,” *Phys. Rev. D* **81**, 123016 (2010) [arXiv:0911.3535 [astro-ph.HE]].
- [56] S. Postnikov, M. Prakash and J. M. Lattimer, “Tidal Love Numbers of Neutron and Self-Bound Quark Stars,” *Phys. Rev. D* **82**, 024016 (2010) [arXiv:1004.5098 [astro-ph.SR]].
- [57] J. M. Lattimer and M. Prakash, “The Equation of State of Hot, Dense Matter and Neutron Stars,” *Phys. Rept.* **621**, 127-164 (2016) [arXiv:1512.07820 [astro-ph.SR]].
- [58] B. P. Abbott *et al.* [LIGO Scientific and Virgo Collaborations], “GW170817: Observation of Gravitational Waves from a Binary Neutron Star Inspiral”, *Phys. Rev. Lett.* **119**, 161101 (2017) [arXiv:1710.05832 [gr-qc]].
- [59] V. Cardoso, M. Kimura, A. Maselli and L. Senatore, “Black Holes in an Effective Field Theory Extension of General Relativity,” *Phys. Rev. Lett.* **121**, 251105 (2018) [arXiv:1808.08962 [gr-qc]].
- [60] P. Pani, “I-Love-Q relations for gravastars and the approach to the black-hole limit,” *Phys. Rev. D* **92**, no.12, 124030 (2015) [erratum: *Phys. Rev. D* **95**, 049902 (2017)] [arXiv:1506.06050 [gr-qc]].
- [61] N. Uchikata, S. Yoshida and P. Pani, “Tidal deformability and I-Love-Q relations for gravastars with polytropic thin shells,” *Phys. Rev. D* **94**, 064015 (2016) [arXiv:1607.03593 [gr-qc]].
- [62] G. Pappas and T. A. Apostolatos, “Multipole Moments of numerical spacetimes,” [arXiv:1211.6299 [gr-qc]].
- [63] G. Pappas and T. A. Apostolatos, “Revising the multipole moments of numerical spacetimes, and its consequences,” *Phys. Rev. Lett.* **108**, 231104 (2012) [arXiv:1201.6067 [gr-qc]].
- [64] I. Harry and T. Hinderer, “Observing and measuring the neutron-star equation-of-state in spinning binary neutron star systems,” *Class. Quant. Grav.* **35**, 145010 (2018) [arXiv:1801.09972 [gr-qc]].
- [65] F. D. Ryan, “Spinning boson stars with large selfinteraction,” *Phys. Rev. D* **55**, 6081-6091 (1997)
- [66] F. D. Ryan, “Accuracy of estimating the multipole moments of a massive body from the gravitational waves of a binary inspiral,” *Phys. Rev. D* **56**, 1845-1855 (1997)
- [67] C. A. R. Herdeiro and E. Radu, “Kerr black holes with scalar hair,” *Phys. Rev. Lett.* **112**, 221101 (2014) [arXiv:1403.2757 [gr-qc]].
- [68] D. Baumann, H. S. Chia and R. A. Porto, “Probing Ultralight Bosons with Binary Black Holes,” *Phys. Rev. D* **99**, 044001 (2019) [arXiv:1804.03208 [gr-qc]].
- [69] S. Khan, S. Husa, M. Hannam, F. Ohme, M. Pürrer, X. Jiménez Forteza and A. Bohé, “Frequency-domain gravitational waves from nonprecessing black-hole binaries. II. A phenomenological model for the advanced detector era”, *Phys. Rev. D* **93**, 044007 (2016)

- [arXiv:1508.07253 [gr-qc]].
- [70] A. Bohe, S. Marsat and L. Blanchet, “Next-to-next-to-leading order spin-orbit effects in the gravitational wave flux and orbital phasing of compact binaries”, *Class. Quant. Grav.* **30**, 135009 (2013) [arXiv:1303.7412 [gr-qc]].
- [71] K. G. Arun, A. Buonanno, G. Faye and E. Ochsner, “Higher-order spin effects in the amplitude and phase of gravitational waveforms emitted by inspiraling compact binaries: Ready-to-use gravitational waveforms”, *Phys. Rev. D* **79**, 104023 (2009) Erratum: [*Phys. Rev. D* **84**, 049901 (2011)] [arXiv:0810.5336 [gr-qc]].
- [72] B. Mikoczi, M. Vasuth and L. A. Gergely, “Self-interaction spin effects in inspiraling compact binaries”, *Phys. Rev. D* **71**, 124043 (2005) [astro-ph/0504538].
- [73] Q. Henry, G. Faye and L. Blanchet, “Tidal effects in the gravitational-wave phase evolution of compact binary systems to next-to-next-to-leading post-Newtonian order,” *Phys. Rev. D* **102**, 044033 (2020) [arXiv:2005.13367 [gr-qc]].
- [74] C. K. Mishra, A. Kela, K. G. Arun and G. Faye, Ready-to-use post-Newtonian gravitational waveforms for binary black holes with nonprecessing spins: An update, *Phys. Rev. D* **93**, no. 8, 084054 (2016) [arXiv:1601.05588 [gr-qc]].
- [75] E. Thrane and C. Talbot, “An introduction to Bayesian inference in gravitational-wave astronomy: parameter estimation, model selection, and hierarchical models,” *Publ. Astron. Soc. Austral.* **36**, e010 (2019) [erratum: *Publ. Astron. Soc. Austral.* **37**, e036 (2020)] [arXiv:1809.02293 [astro-ph.IM]].
- [76] J. Veitch *et al.*, “Parameter estimation for compact binaries with ground-based gravitational-wave observations using the LALInference software library”, *Phys. Rev. D* **91**, 042003 (2015) [arXiv:1409.7215 [gr-qc]].
- [77] N. J. Cornish and T. B. Littenberg, “BayesWave: Bayesian Inference for Gravitational Wave Bursts and Instrument Glitches,” *Class. Quant. Grav.* **32**, no.13, 135012 (2015) [arXiv:1410.3835 [gr-qc]].
- [78] T. B. Littenberg, J. B. Kanner, N. J. Cornish and M. Millhouse, “Enabling high confidence detections of gravitational-wave bursts,” *Phys. Rev. D* **94**, no.4, 044050 (2016) [arXiv:1511.08752 [gr-qc]].
- [79] K. Chatziioannou, C. J. Haster, T. B. Littenberg, W. M. Farr, S. Ghonge, M. Millhouse, J. A. Clark and N. Cornish, “Noise spectral estimation methods and their impact on gravitational wave measurement of compact binary mergers,” *Phys. Rev. D* **100**, no.10, 104004 (2019) [arXiv:1907.06540 [gr-qc]].
- [80] N. Uchikata and T. Narikawa, “Prospects for estimating parameters from gravitational waves of superspinar binaries,” [arXiv:2104.12968 [gr-qc]].
- [81] J. Skilling, *Bayesian Analysis* **1**, 833 (2006).
- [82] J. Veitch and A. Vecchio, “Bayesian coherent analysis of in-spiral gravitational wave signals with a detector network”, *Phys. Rev. D* **81**, 062003 (2010) [arXiv:0911.3820 [astro-ph.CO]].
- [83] LIGO Scientific Collaboration, LIGO Algorithm Library - LALSuite, Free Software (GPL), 2018; <https://doi.org/10.7935/GT1W-FZ16>.
- [84] B. P. Abbott *et al.* [LIGO Scientific and Virgo], “GW170608: Observation of a 19-solar-mass Binary Black Hole Coalescence,” *Astrophys. J. Lett.* **851**, L35 (2017) [arXiv:1711.05578 [astro-ph.HE]].
- [85] LIGO Scientific and Virgo Collaborations, 2020, <https://doi.org/10.7935/99gf-ax93>.
- [86] P. Ajith, M. Hannam, S. Husa, Y. Chen, B. Brügmann, N. Dorband, D. Müller, F. Ohme, D. Pollney, C. Reisswig *et al.*, “Inspiral-merger-ringdown waveforms for black-hole binaries with non-precessing spins,” *Phys. Rev. Lett.* **106**, 241101 (2011) [arXiv:0909.2867 [gr-qc]].
- [87] L. Santamaria, F. Ohme, P. Ajith, B. Bruegmann, N. Dorband, M. Hannam, S. Husa, P. Mosta, D. Pollney and C. Reisswig, *et al.* “Matching post-Newtonian and numerical relativity waveforms: systematic errors and a new phenomenological model for non-precessing black hole binaries,” *Phys. Rev. D* **82**, 064016 (2010) [arXiv:1005.3306 [gr-qc]].
- [88] Planck Collaboration: P. A. R. Ade, N. Aghanim, M. I. R. Alves, C. Armitage-Caplan, M. Arnaud, M. Ashdown, F. Atrio-Barandela, J. Aumont, H. Aussel, C. Bacigalupi *et al.*, “Planck 2013 results. I. Overview of products and scientific results,” *Astron. Astrophys.* **571**, A1 (2014) [arXiv:1303.5062 [astro-ph.CO]].
- [89] H. Jeffreys, “Theory of Probability, 3rd edn.” Oxford University Press, 1961.
- [90] R. Abbott *et al.* [LIGO Scientific and Virgo], “GW190814: Gravitational Waves from the Coalescence of a 23 Solar Mass Black Hole with a 2.6 Solar Mass Compact Object,” *Astrophys. J. Lett.* **896**, no.2, L44 (2020) [arXiv:2006.12611 [astro-ph.HE]].
- [91] A. Vijaykumar, N. K. Johnson-McDaniel, R. Kashyap, A. Mukherjee, and P. Ajith, in preparation.